ACADÉMIE
DES SCIENCES
INSTITUT DE FRANCE

Comptes Rendus
Physique

Gabriel Hadjerci, Vincent Bouillaut, Benjamin Miquel, Sébastien Aumaître and Basile Gallet

Radiatively driven convection: diffusivity-free regimes of geophysical and astrophysical flows in the laboratory

Published online: 12 December 2024

Part of Special Issue: Geophysical and astrophysical fluid dynamics in the laboratory
Guest editors: Stephan Fauve (Laboratoire de Physique de l'ENS, CNRS, PSL Research University, Sorbonne Université, Université Paris Cité, Paris, France) and Michael Le Bars (CNRS, Aix Marseille Univ, Centrale Marseille, IRPHE, Marseille, France)

https://doi.org/10.5802/crphys.207

The Comptes Rendus. Physique *are a member of the Mersenne Center for open scientific publishing*
www.centre-mersenne.org — e-ISSN : 1878-1535

ACADÉMIE DES SCIENCES
INSTITUT DE FRANCE

Comptes Rendus. Physique
Published online: 12 December 2024
https://doi.org/10.5802/crphys.207

Review article / *Article de synthèse*

Geophysical and astrophysical fluid dynamics in the laboratory / *Dynamique des fluides géophysiques et astrophysiques au laboratoire*

Radiatively driven convection: diffusivity-free regimes of geophysical and astrophysical flows in the laboratory

La convection engendrée par forçage radiatif, ou comment reproduire en laboratoire les régimes « ultimes » des écoulements géo- et astrophysiques

Gabriel Hadjerci [a], Vincent Bouillaut [b], Benjamin Miquel [c], Sébastien Aumaître [a] and Basile Gallet [*,a]

[a] Université Paris-Saclay, CNRS, CEA, Service de Physique de l'Etat Condensé, 91191 Gif-sur-Yvette, France

[b] Onera Châtillon, 92320, Châtillon, France

[c] Univ Lyon, CNRS, Ecole Centrale de Lyon, INSA Lyon, Université Claude Bernard Lyon 1, LMFA, UMR5509, 69130, Ecully, France

E-mail: basile.gallet@cea.fr (B. Gallet)

Abstract. We consider the turbulent heat transport induced by thermal convection. The widespread belief is that the transport properties of the turbulent flow should be independent of the tiny molecular diffusivities for asymptotically strong driving, but the associated "ultimate" scaling regime proves challenging to observe experimentally using standard convection cells (Rayleigh–Bénard geometry). We thus recently introduced an alternate experimental setup where convection is driven radiatively, with internal heating within the lower region of the body of fluid. This setup naturally leads to the ultimate regime of thermal convection. We then discuss how adding global rotation to the experimental setup has led to the first laboratory observation of the diffusivity-free regime of rapidly rotating turbulent convection, also known as the "geostrophic turbulence" scaling regime.

Résumé. Cet article traite du transport turbulent de chaleur engendré par convection thermique. Si la croyance dominante est que les propriétés de transport de l'écoulement turbulent sont asymptotiquement indépendantes des diffusivités moléculaires du fluide, ce régime dit « ultime » semble difficile à mettre en évidence dans les expériences traditionnelles de laboratoire (dispositif de Rayleigh–Bénard). Nous avons donc récemment développé un dispositif de convection par chauffage radiatif, dans lequel le fluide est chauffé en volume dans sa partie inférieure. Nous montrerons comment ce dispositif conduit naturellement à l'observation du régime ultime de convection thermique en laboratoire. Nous décrirons ensuite l'ajout

* Corresponding author

d'une rotation globale à ce dispositif expérimental, ingrédient important des écoulements géophysiques et astrophysiques. Nous montrerons en particulier comment ce dispositif a permis la première observation expérimentale du régime ultime de convection en rotation rapide, dit régime de « turbulence géostrophique ».

Keywords. turbulent convection, geophysical and astrophysical fluid dynamics, rotating turbulence.

Mots-clés. convection turbulente, dynamique des fluides géophysiques et astrophysiques, turbulence en rotation.

Funding. This research is supported by the European Research Council under grant agreement FLAVE 757239.

Manuscript received 24 May 2024, revised 12 September 2024, accepted 13 September 2024.

Thermal convection is a key driver of geophysical and astrophysical flows, be it in stellar and planetary interiors, in exoplanetary atmospheres, in the Earth ocean and in the oceans of outer solar system satellites [1–7]. In these various contexts the convective flow is typically strongly turbulent. A standard modeling assumption thus consists in assuming that the zeroth-law of turbulence applies [8]: the large-scale quantities should be related in a way that does not involve the tiny molecular diffusivities (of momentum, heat, or tracer concentration).

The vast majority of the physics literature on thermal convection focuses on the Rayleigh–Bénard (RB) convection setup, where a layer of fluid is sandwiched between a hot bottom plate and a cool top one. While arguably the simplest setup from a theoretical point of view, RB convection appears to be a questionable model for geophysical and astrophysical flows. Indeed, the diffusivity-free argument above suggests that the turbulent heat flux should be related to the temperature difference between the two plates in a way that does not involve the molecular diffusivities. As discussed in Section 1, this corresponds to the Nusselt number Nu (dimensionless heat flux) increasing with the Rayleigh number Ra (dimensionless temperature difference) as $Nu \sim Ra^{\gamma}$, with $\gamma = 1/2$. While the precise value of the exponent γ remains debated for the highest Ra achieved in laboratory experiments, all measured values lie in the range $0.26 \leq \gamma \leq 0.38$ [9–15], that is, the measured exponent is always strictly less than $1/2$ (restricting attention to smooth top and bottom plates, see below).

The lower value for the exponent γ results from the boundary layers adjacent to the top and bottom plates, which throttle the heat flux throughout the entire cell. Based on this observation, several alternate setups have been designed to mitigate the role of the boundary layers and observe diffusivity-free convection in the laboratory: convection in tall vertical channels [16–20], Rayleigh–Bénard convection with rough boundaries [21–27], and radiatively driven convection [28–30]. After briefly reviewing the results obtained using the first two experimental setups, we discuss radiatively driven convection in greater detail, with an emphasis on its ability to reproduce various diffusivity-free regimes of geophysical and astrophysical relevance.

In Section 1 we introduce standard RB convection together with the standard theoretical predictions for the exponent γ, before briefly reviewing results obtained in tall channel experiments and in RB experiments with rough boundaries. We introduce the radiatively driven convection setup in Section 2, focusing first on the observation of the diffusivity-free regime of non-rotating convection. In Section 3 we discuss the influence of rapid global rotation and the laboratory realization of the geostrophic turbulence scaling regime – the diffusivity-free or "ultimate" regime of rapidly rotating convection – using a rotating radiatively driven convection experiment. We conclude in Section 4.

1. A primer on Rayleigh–Bénard convection

The RB setup is sketched in Figure 1(a): a layer of fluid of height H lies between a warm bottom plate maintained at temperature $T_0 + \Delta T$ and a cool top plate maintained at temperature T_0. At the theoretical level, the layer can be considered infinite or periodic in the horizontal directions.

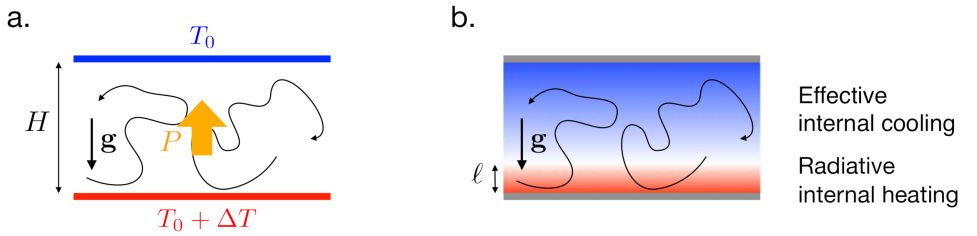

Figure 1. Rayleigh–Bénard convection (a) consists of a layer of fluid sandwiched between a hot bottom plate and a cool top one, the plates being kept at fixed temperatures. One typically measures the emergent heat flux. By contrast, radiatively driven convection (b) is powered by radiative heating and effective internal cooling, the boundaries being thermally insulated. One typically measures the emergent vertical temperature drop.

The density depends linearly on temperature T, $\rho = \rho_0[1 - \alpha(T - T_0)]$. Following the traditional Boussinesq approximation, the other coefficients characterizing the fluid's properties are independent of temperature: kinematic viscosity ν, thermal diffusivity κ, thermal expansion coefficient α, specific heat capacity C, etc. One can also show that, for small enough temperature drop ΔT, the density variations need only be included in the expression of the weight of the fluid element [31], while the velocity field can be considered incompressible (divergence-free).

There are two dimensionless control parameters for such Boussinesq RB convection. The Rayleigh number,

$$Ra = \frac{\alpha g \Delta T H^3}{\kappa \nu}, \tag{1}$$

characterizes the intensity of the thermal driving as compared to diffusive effects. The Prandtl number,

$$Pr = \frac{\nu}{\kappa}, \tag{2}$$

characterizes the relative importance of viscosity and thermal diffusion. To some extent, Pr can be considered constant for a given fluid: $Pr \simeq 7$ for water around room temperature, $Pr \simeq 3 \times 10^{-2}$ for liquid metals, $Pr \ll 1$ in typical astrophysical settings.

At low Rayleigh number the fluid remains motionless, with warm fluid sitting below heavier cooler fluid and heat diffused from the bottom to the top plate. However, this situation becomes unstable at stronger driving amplitude, that is, above a threshold value Ra_c of the Rayleigh number. Cellular motion arises, the system trying to reach the lower-potential-energy state where heavy fluid lies below lighter fluid. After reaching saturation, the flow is typically steady slightly above threshold and destabilizes at higher values of Ra through secondary instabilities. At very high Ra the flow is turbulent. As compared to the diffusive state, convective motion greatly enhances the heat transport from the bottom to the top plate. Indeed, fluid elements receive heat near the bottom plate, rise, and eventually deposit the heat at the cool top plate. Such convective transport is very efficient and greatly dominates over diffusive transport for large Rayleigh number, $Ra \gg Ra_c$. The overall efficiency of the heat transport can be characterized using the mean heat flux P transferred across any horizontal surface $z = \text{const.}$ in statistically steady state. Non-dimensionalizing this heat flux P with the diffusive heat flux of the steady motionless state leads to the Nusselt number:

$$Nu = \frac{PH}{\rho_0 C \kappa \Delta T}. \tag{3}$$

The heat flux P is a central quantity of the convection system, related to most other global quantities of interest. The heat flux P is directly proportional to the rate of mechanical energy input into the system, which in statistically steady state is balanced by viscous dissipation. The heat flux P is also related to the input of buoyancy variance into the system, the latter being balanced by turbulent mixing. A significant fraction of the research on thermal convection has thus been devoted to the determination of the scaling behavior of Nu as a function of Ra and Pr in controlled laboratory experiments and numerical simulations. The goal is to determine the behavior of Nu at asymptotically large Ra, and one typically seeks a power-law of the form $Nu \sim Ra^{\gamma} Pr^{\chi}$. However, two competing theoretical predictions have been put forward for the values of the exponents γ and χ.

1.1. *"Classical" scaling regime*

The classical theory is based on the observation that the temperature is almost homogeneous in the interior of high-Ra RB convection, with sharp gradients located within the boundary layers adjacent to the top and bottom plates. The interpretation is that the bulk turbulent flow efficiently mixes temperature, hence the isothermal profile in the interior of the domain. However, fluid hardly moves (in the vertical direction) near the top and bottom plates, hence the existence of boundary layers connecting the isothermal interior with the boundary values of the temperature field. Because the fluid hardly moves near the boundaries, heat transfer is dominated by diffusion in the boundary layers. Assuming that diffusive transfer across the boundary layers throttles the overall heat flux, we estimate P as

$$P \sim \frac{\rho_0 C \kappa \Delta T}{\delta} \tag{4}$$

where δ denotes the thickness of the thermal boundary layer. The boundary layer thickness δ can be deduced from a marginal stability argument initally articulated by Howard [32]: the Rayleigh number based on δ is comparable to the threshold Rayleigh number for thermal convection,

$$Ra^{(\delta)} = \frac{\alpha g \Delta T \delta^3}{\kappa \nu} \simeq Ra_c \,. \tag{5}$$

The rationale is the following: if δ were much thinner than (5), the boundary layer could grow diffusively. However, if δ were greater than the estimate (5), the boundary layer itself would become convectively unstable. The boundary layer would then spontaneously erode and δ would decrease. The conclusion is that, in statistically steady state, the boundary layer thickness δ is given by (5), where Ra_c is a constant number, typically of the order of 10^3. Substituting the estimate (5) for δ into equation (4) yields, after multiplication by $H/(\rho_0 C \kappa \Delta T)$:

$$Nu \sim \frac{H}{\delta} \sim Ra^{1/3} \,, \tag{6}$$

that is, $\gamma = 1/3$ and $\chi = 0$.

1.2. *Diffusivity-free or "ultimate" scaling regime*

The competing theoretical prediction, attributed to Spiegel and Kraichnan [33–35], is based on the zeroth law of turbulence. In a loose sense, the law states that large-scale quantities in a turbulent flow are related in a way that does not involve the tiny molecular diffusivities. In the present situation, one seeks a scaling relation between P and ΔT that does not involve κ nor ν. Start from the general scaling relation:

$$Nu \sim Ra^{\gamma} Pr^{\chi} \,. \tag{7}$$

Demanding that P and ΔT be related in a way that does not involve ν leads to $\chi = \gamma$ so that:

$$Nu \sim (Ra \times Pr)^{\gamma} . \tag{8}$$

Remembering that κ appears at the denominator of Nu, the only way for P and ΔT to be related in a way that does not involve κ is to have the right-hand side of (8) be inversely proportional to κ. We conclude that:

$$Nu \sim \sqrt{Ra \times Pr}, \tag{9}$$

that is, $\gamma = \chi = 1/2$. The scaling relation (9) is sometimes attributed to E.A. Spiegel [33, 34], who is said to have put forward the idea in an astrophysical context without publishing it. In the meantime, his then postdoc advisor R.H. Kraichnan published a similar prediction, up to logarithmic corrections [35]. Kraichnan's approach consists in arguing that the boundary layers of the classical theory above should become turbulent at sufficiently high Rayleigh number. He assumes that a turbulent velocity boundary layer arises at large Ra, and that this turbulent boundary layer resembles those of standard shear flow turbulence, with a logarithmic layer and a viscous sublayer in the immediate vicinity of the boundary. This structure for the boundary layer leads to the prediction (9) divided by a logarithmic correction in Rayleigh number. In the physics and fluid dynamics community the scaling-law (9) is often referred to as the "ultimate" scaling regime of convection, possibly because according to Kraichnan the velocity boundary layers should ultimately become turbulent as Ra increases. In the astrophysics community, (9) is referred to as the mixing-length scaling-law and is believed to be the relevant scaling-law for the extreme parameter regimes of astrophysical flows.

1.3. *Non-standard RB setups to achieve the diffusivity-free regime*

As discussed above, for standard RB convection the measured heat transport exponent γ is significantly smaller than 1/2 as a result of the throttling effect of the boundary layers. Insightful alternate experimental setups were therefore designed to mitigate the role of the boundary layers.

Among the different strategies that have been deployed, one option consists in studying convection in a narrow vertical channel connecting two large reservoirs of cool and warm fluid at top and bottom, respectively. The goal is to have a tall enough channel for the system to be considered virtually infinite in the vertical direction. One then seeks a relation between the heat flux and the bulk vertical temperature *gradient*. One difficulty is then to identify the relevant lengthscale to define the associated dimensionless numbers. In early experiments, Gibert et al. [16] employed a mixing-length based on the ratio of the temperature fluctuations to the temperature gradient. With this definition, the resulting Nusselt number increases with the square root of the resulting Rayleigh number, indicating diffusivity-free scaling. However, it was further shown in Ref. [19, 20] that the mixing-length scales as the width L of the domain: as a consequence, the turbulent heat flux in tall vertical channels is related to the vertical temperature gradient in a way which does not involve the molecular diffusivities, but which explicitly involves the width L of the domain. While such a diffusivity-free regime is a significant achievement at the fundamental level, this strong dependence on lateral width makes the setup ill-suited as a model of geophysical or astrophysical flows. Indeed, the latter flows typically correspond the limit $L \to \infty$ for fixed height H, opposite to the limit considered in tall vertical channels. As an alternative, one may try to reach this $L \to \infty$ regime while avoiding the top and bottom boundary layers by simulating thermal convection numerically using periodic boundary conditions in the vertical direction. However, in such numerical simulations the heat flux diverges as a result of the emergence of "elevator" modes. The conclusion seems to be that convective flows in the horizontally infinite plane layer are always aware of the height H of the layer.

An alternative strategy to disrupt the throttling effect of the boundaries consists in replacing the smooth top and bottom boundaries by rough plates. This approach leads to an increased value for the exponent γ. The latter reaches $1/2$ in some experiments, the precise value of the exponent and of the prefactor depending on details of the roughness elements (see e.g. Refs. [22, 27]). The exponent was observed to revert to a more modest value at higher Rayleigh number in some experiments and idealized numerical simulations [27, 36, 37], with a high-Ra value close to $1/3$, when the thin boundary layer follows the roughness elements. Multiscale roughness (a fractal boundary) may be a way to disrupt the boundary layers up to arbitrarily high Rayleigh number [38].

Additionally, in other experiments with regular roughness elements the exponent remains close to $1/2$ up to the highest Ra achieved experimentally [24]. It could be that the relaxation to $\gamma = 1/3$ occurs at even higher Ra, or that the roughness has helped the system transition to an ultimate scaling regime. As compared to Kraichnan's theory, this ultimate regime would be characterized by a prefactor that depends on details of the roughness of the two plates.

In the following section we discuss radiative heating as an alternate way to observe diffusivity-free thermal convection, in a way that survives the limit $L \to \infty$. As compared to the use of rough plates, radiative heating comes with its own advantages and challenges. For instance, rough plates are much simpler to implement in a pre-existing RB experiment than radiative heating. On the other hand, radiative heating is arguably simpler to handle at the theoretical level: in contrast to rough-plate convection, radiatively driven convection is amenable to linear stability analysis with a well-defined threshold Rayleigh number for the emergence of convection. Additionally, the high-Ra exponent does not depend on the details of the structure of a rough boundary. In particular, radiatively driven convection is easily simulated numerically using high-accuracy pseudo-spectral solvers [39].

2. Radiatively driven convection

2.1. *An experimental setup to bypass the boundary layers*

One way to mitigate the throttling effect of the boundary layers is to input the heat predominantly beyond the latter, directly into the bulk turbulent flow as represented in Figure 1(b). We put this idea into practice by employing radiative heating in the experimental setup described thereafter and sketched in Figure 2. A cylindrical tank of radius 10cm with a transparent bottom plate contains a mixture of water and carbon-black dye. A powerful spotlight shines at the tank from below, and the absorption of light by the dye induces radiative heating. Following Beer–Lambert's law, the light intensity decreases exponentially with height z measured from the bottom of the tank, over an e-folding absorption scale ℓ, and so does the internal heat source. The absorption length ℓ is easily tuned through the concentration of the dye. For large dye concentration the heat source is localized in the immediate vicinity of the bottom plate, with ℓ much smaller than the thickness of the velocity and temperature boundary layers. Such a heat source is similar to an imposed bottom heat flux; we thus expect a throttling effect associated with the presence of the bottom boundary layer, in a similar fashion to RB convection. By contrast, using lower dye concentration, ℓ can be made much thicker than the boundary layers. The heat is then directly input into the bulk turbulent flow, bypassing the high thermal impedance of the boundary layers.

Achieving a clean exponentially decreasing heat source inside the tank requires a few precautions. The light emitted by the spotlight first travels through a water-cooled water tank which efficiently filters out infrared radiation. In addition, we use carbon-black dye, which absorbs visible light at the same rate regardless of wavelength. Assuming a horizontally homogeneous light flux, the internal radiative heat source inside the tank reads $(P/\ell)\, e^{-z/\ell}$, where P denotes the energy

flux radiated by the spotlight in the form of visible light (P is expressed in units of W.m^{-2}). Describing the experiment within the framework of the Boussinesq approximation, the governing equation for the temperature $T(x,y,z,t)$ inside the tank reads [28]:

$$\partial_t T + \mathbf{u}\cdot\nabla T = \kappa\nabla^2 T + \frac{P}{\rho_0 C\ell} e^{-z/\ell}, \tag{10}$$

where $\mathbf{u}(x,y,z,t)$ denotes the velocity field.

2.2. *Secular heating and effective internal cooling*

Cooling the fluid through the top surface would necessarily introduce boundary layers, which would negate the careful efforts deployed to bypass these layers on the heating side [40]. Instead, we resort to secular heating as an analog to internal cooling. Assuming adiabatic boundary conditions, one can average equation (10) over space to obtain the evolution equation for the spatially averaged temperature $\overline{T}(t)$:

$$\frac{\mathrm{d}\overline{T}}{\mathrm{d}t} = \frac{P}{\rho_0 CH}\left(1 - e^{-H/\ell}\right) \simeq \frac{P}{\rho CH}, \tag{11}$$

where H denotes the height of fluid and we have assumed $\ell \ll H$ to obtain the last equality. Equation (11) indicates that the mean temperature inside the tank increases linearly with time, because heat is supplied at a constant rate. To investigate the internal temperature structure

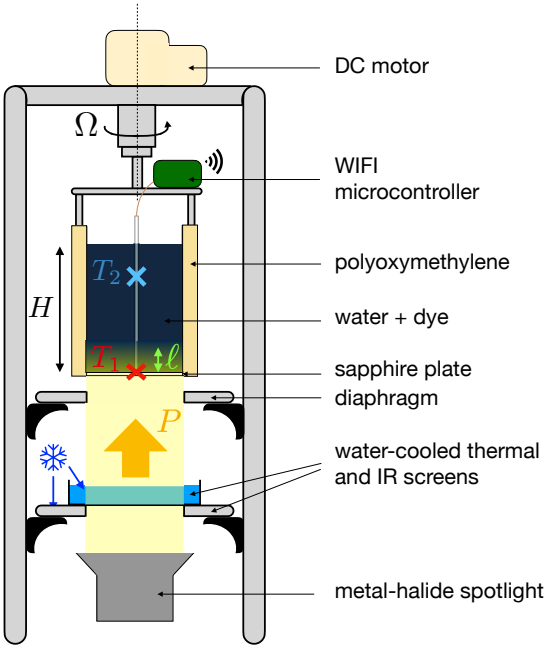

Figure 2. Radiatively driven convection in the laboratory. A powerful spotlight shines from below at a mixture of water and dye. The resulting internal heat source decreases exponentially with height over the absorption length ℓ, delivering a total heat flux P. With the goal of studying both rotating and non-rotating convection, the cylindrical tank is attached from above to a DC motor. Two thermocouples T_1 and T_2 measure the vertical temperature drop.

within the fluid, one can introduce the variable $\theta(x,y,z,t) = T(x,y,z,t) - \overline{T}(t)$ which represents the temperature fluctuations around the spatial average and obeys:

$$\partial_t \theta + \mathbf{u}\cdot\nabla\theta = \kappa\Delta\theta + \frac{P}{\rho_0 C}\left(\frac{e^{-z/\ell}}{\ell} - \frac{1}{H}\right). \tag{12}$$

In the parentheses is the radiative heat source, together with an effective uniform heat sink that balances the heat source over space average. Secular heating thus induces an effective uniform internal cooling in equation (12), offering a way to avoid any boundary layer on the cooling side. As for the traditional Boussinesq set of equations, equation (12) is coupled to the incompressible Navier–Stokes equation, the latter including a buoyancy term proportional to θ. Solutions to this set of equations reach a statistically steady state in the long time limit, which we wish to characterize. To wit, we measure a first temperature $T_1(t)$ using a thermocouple touching the bottom plate of the tank, and a second temperature $T_2(t)$ using second probe placed in the bulk of the fluid volume (at $z = H/2$ for non-rotating experiments and at $z = 3H/4$ for rotating experiments). At the outset of an experiment we fill the tank up to a height H with cold water mixed with carbon-black dye, before turning on the spotlight. While the two temperature signals drift with time as a result of secular heating, after an initial transient phase the temperature drop $T_1(t) - T_2(t)$ reaches a statistically steady state. We denote as ΔT the resulting time-averaged temperature drop, measured in the statistically steady phase. Examples of timeseries $T_1(t)$ and $T_2(t)$ can be found in Refs. [28, 30]. Because of the large body of fluid, the rise of the mean temperature is fairly slow. This allows for an extended statistically steady state lasting many turnover times, while having a mean temperature that remains close to room temperature. The Boussinesq approximation is very well satisfied in this quasi-stationary state (as further confirmed by the good agreement with numerical simulations in Refs. [28, 30]).

The knowledge of both the flux and the temperature drop gives us access to the Rayleigh number Ra and Nusselt number Nu. While these two parameters allow for a clear comparison with the RB literature, none of them is a true control parameter of our experiment. We thus also define the flux-based Rayleigh number Ra_P as:

$$Ra_P = Nu \times Ra = \frac{\alpha g P H^4}{\rho C \kappa^2 \nu}. \tag{13}$$

Although not independent from Ra and Nu, the flux-based Rayleigh number Ra_P is a true control parameter of the experiment, in the sense that it does not depend on the response of the flow and hence can be specified at the outset of an experimental run.

2.3. *Experimental observation of the ultimate scaling regime*

A suite of experiments typically consists in fixing the value of the dimensionless absorption length ℓ/H and performing experimental runs for various heights H of fluid. Lepot et al. [28] initially focused on two limiting situations of interest: $\ell/H < 10^{-4}$, where the heating is similar to fixed flux RB convection, and $\ell/H = 0.05$, which is sufficient to bypass the boundary layers. The resulting plots Nu versus Ra clearly confirm the intuition discussed above: $\ell/H < 10^{-4}$ leads to the classical regime of convection, with a best-fit exponent $\gamma = 0.31$, close to 1/3. By contrast, $\ell/H = 0.05$ leads to a best-fit exponent $\gamma = 0.54$, very close to the prediction 1/2 of the ultimate scaling regime. The experiment thus provides an efficient way to bypass the boundary layers and observe ultimate scaling regimes of convection in the laboratory.

The transition between the two regimes was further characterized by Bouillaut et al. [29], who performed additional experiments for various values of ℓ/H. The resulting dataset is shown in the (Ra, Nu) plane in Figure 3. Low ℓ/H data are compatible with the classical scaling regime, while high ℓ/H data are compatible with the ultimate or diffusivity-free scaling prediction.

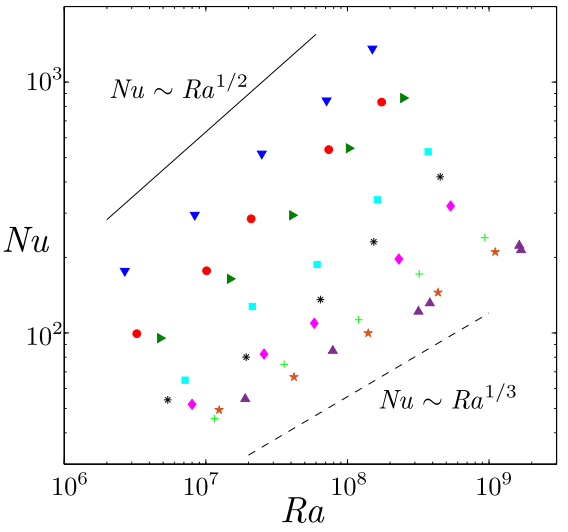

Figure 3. Nusselt number as a function of the Rayleigh number for various values of the absorption length ℓ. At fixed Ra, the Nusselt number increases with ℓ/H. Symbols are $\triangle$: $\ell/H = 5\times10^{-6}$ m; $\star$: $\ell/H = 0.0052$; $+$: $\ell/H = 0.0030$; $\Diamond$: $\ell/H = 0.0060$; $*$: $\ell/H = 0.012$; $\square$: $\ell/H = 0.024$; $\triangleright$: $\ell/H = 0.048$; $\bigcirc$: $\ell/H = 0.05$; $\triangledown$: $\ell/H = 0.096$. The solid and dashed lines are eyeguides.

Additionally, one observes that the prefactor of the scaling law depends on the dimensionless absorption length ℓ/H. Bouillaut et al. [29] introduce a simple "roll" model to predict the dependence of Nu on ℓ/H. The main idea consists of following the trajectory of a fluid element traveling at the periphery of the large-scale roll-shaped mean circulation of the turbulent flow. The fluid heats up as it travels within the radiatively heated region near the bottom of the tank, subsequently sharing that excess heat as it rises into the bulk region (see Ref. [29] for a detailed description of the model). Assuming that the speed of the mean circulation scales as a free-fall velocity, Bouillaut et al. [29] conclude that the Nusselt number should be proportional to ℓ/H for fixed Ra in the diffusivity-free regime. One thus expects data points pertaining both to the classical scaling regime and the ultimate scaling regime to collapse onto a single master curve when plotting $Nu(\ell/H)^2$ as a function of $Ra(\ell/H)^6$. Indeed, the classical scaling regime $Nu \sim Ra^{1/3}$corresponds to $Nu(\ell/H)^2 \sim [Ra(\ell/H)^6]^{1/3}$, while the ultimate scaling regime $Nu \sim (\ell/H)Ra^{1/2}$ corresponds to $Nu(\ell/H)^2 \sim [Ra(\ell/H)^6]^{1/2}$. As shown in Figure 4, this representation indeed leads to a good collapse of the data onto a single master curve, which provides a validation of the dependence of Nu on ℓ/H predicted by Bouillaut et al. [29].

For large enough $Ra(\ell/H)^2$ the boundary layers are bypassed. However, there is still a sub-dominant amount of heat that is directly input into the boundary layers. As inferred by Bouillaut et al. [29] through a refinement of their roll model and further confirmed using numerical simulation in Ref. [41], this process affects the high-Prandtl-number regime with no-slip boundary conditions, whereas it is negligible for low Prandtl number or stress-free boundary conditions (regardless of Pr).

2.4. *Maximal heat transport efficiency?*

The quest for the ultimate regime of thermal convection is deeply connected to the conjecture that turbulent convection may self-organize to maximize the heat transport. This idea, initially

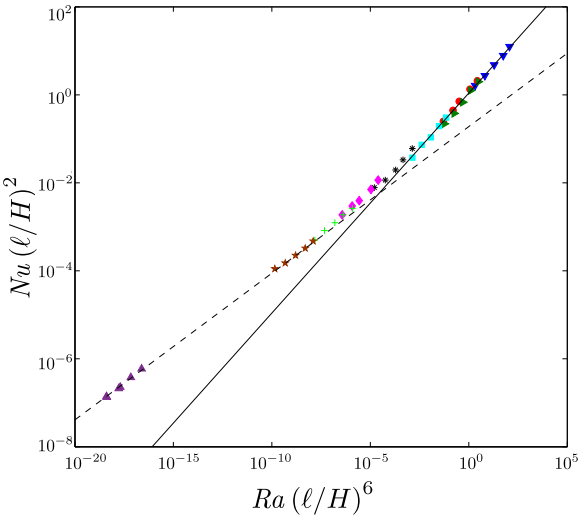

Figure 4. Rescaled Nusselt number as a function of the rescaled Rayleigh number, for various values of the absorption length ℓ (same symbols as Figure 3). The data indicate a clear transition from an exponent $\gamma = 1/3$ (dashed line) to an exponent $\gamma = 1/2$ (solid line).

put forward by Malkus [42], was addressed at a more mathematical level by Howard [32], who solved the associated variational problem and obtained an upper bound on the Nusselt number of the form $Nu \simeq Ra^{1/2}$, that is, $\gamma \leq 1/2$ (see also Refs. [43, 44]). This bound only holds for the RB setup, however, and it turns out that radiatively driven convection allows for higher values of the exponent γ. Specifically, an analytical high-Rayleigh-number asymptotic solution to convection driven by internal heat sources and sinks was derived in Ref. [45]. The asymptotic solution achieves heat transport beyond the ultimate scaling regime, with $Nu \sim Ra$. While this asymptotic solution is observed in 2D DNS of radiatively driven convection with suitable boundary conditions [45], it is not realized in 3D DNS nor is it realized in the above-mentioned laboratory experiments. Instead, as intuition suggests, the high-Reynolds-number experimental flow is strongly turbulent and does not realize the idealized laminar flow solution computed by [45]. Spurred by this observation, the bounding procedure was subsequently refined in Ref. [46] by distinguishing between laminar versus turbulent branches of solutions (the bounding procedure was also extended to arbitrary distributions of heat sources and sinks, see Ref. [47]). The authors of Ref. [46] show that, for branches of flow solutions that obey the zeroth-law of turbulence (viscous energy dissipation rate independent of viscosity), the scaling exponent γ is bounded from above by $1/2$ at asymptotically high Ra (in other words, only non-turbulent flows can achieve $\gamma > 1/2$). Because the experimental data reviewed above are compatible with $\gamma = 1/2$, one concludes that radiatively driven convection maximizes the heat transport over turbulent flow solutions [46].

3. Radiatively driven rotating convection: observation of the diffusivity-free scaling regime

Radiatively driven convection is an appealing experimental setup to include the various additional ingredients of geophysical and astrophysical flows, such as global rotation or magnetic

field. The goal is to achieve the diffusivity-free regimes that are typically invoked when modeling geophysical and astrophysical convective flows, but remain out of reach of RB experiments [48–50] (see Ref. [51] for the rotating version of the "classical" scaling regime discussed in Section 1.1). As compared to RB convection using plates with regular roughness, an appealing aspect of radiatively-driven convection is that it comes with no preferred scale in the horizontal directions. This feature is particularly desirable when convection is subject to rotation or magnetic field, because these two ingredients tend to select a specific horizontal scale. The competition between the roughness scale of the plate and the preferred scale of rotating/magnetic convection may then complicate the analysis (see the careful studies in Refs. [52, 53]). At the numerical level, rotating convection with periodic boundary conditions in the vertical direction [54] is also subject to "elevator modes" (see e.g. Ref. [55] for a discussion).

3.1. *Rapid rotation: the geostrophic turbulence scaling regime*

We consider convection subject to global rotation around the vertical axis z, restricting attention to astro- and geophysically relevant cases where centrifugal effects are negligible. Rotation then enters the governing equations through the addition of the Coriolis term in the Navier–Stokes equation. The rotation rate Ω is an additional dimensional control parameter of the system, its dimensionless counterpart being the Ekman number $E = \nu/(2\Omega H^2)$. The Nusselt number is a function of the three control parameters of the system:

$$Nu = \mathscr{F}(Ra_P, Pr, E)\,, \tag{14}$$

where $\mathscr{F}$ generically denotes the existence of some scaling relation. Due to the presence of an additional dimensionless parameter as compared to the non-rotating case, one cannot derive scaling predictions solely based on the dimensional analysis arguments introduced in Section 1.

Additional progress can be made by focusing on the rapidly rotating regime, $E \ll 1$. In this asymptotic regime, the critical (flux-based) Rayleigh number for the emergence of convection increases as $Ra_P^{(c)} \sim E^{-4/3}$. Crucially, Julien and Knobloch performed an asymptotic reduction of the rotating Boussinesq system [56, 57]. The resulting reduced model was extensively studied by means of numerical simulations [58, 59]. Most importantly, the reduced model indicates that, in the asymptotic regime of rapid rotation, the control parameter is the supercriticality $Ra_P/Ra_P^{(c)} \sim Ra_P E^{4/3}$. That is, instead of Ra_P, Pr and E appearing independently in the equations, only Pr and the grouping $Ra_P E^{4/3}$ arise in the reduced set of equations describing the asymptotic rapidly rotating regime. The Nusselt number thus depends only on these two control parameters:

$$Nu = \mathscr{F}(Ra_P E^{4/3}, Pr)\,, \tag{15}$$

provided rotation is fast enough. The next step consists in combining equation (15) with the dimensional analysis arguments put forward in Section 1. Specifically, assuming the existence of a diffusivity-free regime of rapidly rotating convection amounts to demanding that the function $\mathscr{F}$ in (15) be such that κ and ν can be crossed out on both sides of the equation. This leads to the "geostrophic turbulence" (GT) scaling regime of rapidly rotating convection [58]:

$$Nu \sim Ra_P^{3/5} E^{4/5} Pr^{-1/5}\,. \tag{16}$$

To our knowledge, this scaling prediction was initially put forward in Ref. [1] based on phenomenological arguments. In the context of rapidly rotating RB convection, it is more often cast in terms of the standard temperature-based Rayleigh number. Substituting $Ra_P = Nu \times Ra$ into (16):

$$Nu \sim Ra^{3/2} E^2 Pr^{-1/2}\,. \tag{17}$$

3.2. *Experimental realization*

As reported in Ref. [30], the radiatively driven convection setup can be adapted to include global rotation, allowing for an experimental realization of the insightful but somewhat academic numerical setup considered in Ref. [60]. Because no cooling is required and radiative heating is contactless, one can simply attach the tank from above to a motor and spin it around the vertical axis, see Figure 2. We perform the temperature measurements in the rotating frame, using thermocouples located on the axis of the cylinder and connected to a microcontroller. The tank is filled with cool water before rotation is turned on at a constant rate Ω. After a waiting phase of at least ten minutes, allowing for the fluid to settle in solid body rotation, we turn on the spotlight. The dimensional control parameters are varied in the range $H \in [10, 25]$cm and $\Omega \leq 85$rpm, to avoid centrifugal effects. Specifically, suites of experiments were performed in Ref. [30] with fixed height H of fluid and various values of the rotation rate Ω, for two values of the dimensionless absorption length, $\ell/H = 0.024$ and $\ell/H = 0.048$ (see Ref. [30] and the associated supplementary information for tables of parameter values and estimates of the negligible centrifugal effects).

A convenient way to plot the resulting dataset consists in introducing diffusivity-free parameters. The diffusivity-free flux-based Rayleigh number is defined as $\mathscr{R} = Ra_P E^3/Pr^2$, while the diffusivity-free Nusselt number is defined as $\mathscr{N} = NuE/Pr$. These two dimensionless combinations do not involve κ nor ν. If the system indeed achieves diffusivity-free convection, then the entire dataset should collapse onto a master curve in the $(\mathscr{R}, \mathscr{N})$ plane. Additionally, if this diffusivity-free regime is the GT regime (16), then the master curve must be a power-law $\mathscr{N} \sim \mathscr{R}^{3/5}$ (as obtained by substituting $Nu = \mathscr{N} Pr/E$ and $Ra_P = \mathscr{R} Pr^2/E^3$ into (16)).

The entire dataset collected by [30] is shown in Figure 5 in the $(\mathscr{R}, \mathscr{N})$ plane. The dataset does collapse onto a master curve, with two distinct power-law behaviors. For larger values of $\mathscr{R}$, the master curve agrees well with a power-law $\mathscr{N} \sim \mathscr{R}^{1/3}$, which corresponds to the ultimate regime of non-rotating convection (9) recast in terms of $\mathscr{N}$ and $\mathscr{R}$. By contrast, for lower values or $\mathscr{R}$ (say for $\mathscr{R} \lesssim 3 \times 10^{-7}$) the data agrees well with the GT scaling prediction $\mathscr{N} \sim \mathscr{R}^{3/5}$. We conclude that radiatively driven convection transitions from the ultimate regime of non-rotating convection to the ultimate regime of rapidly rotating convection as rotation increases. To facilitate comparison with numerical studies [58, 60–62], Hadjerci et al. [63] show that the transition value $\mathscr{R} \simeq 3 \times 10^{-7}$ to enter the GT regime corresponds to a transition value of approximately 0.03 for the convective Rossby number, within the expected range [64]. That being said, the scatter around the master curve is arguably greater in the crossover region between the two asymptotic regimes, which suggests the possible existence of an intermediate regime involving the diffusivities.

Beyond the sole heat transfer, the GT regime comes with scaling predictions for the temperature fluctuations, the flow speed and the horizontal scale of the flow [64]. Radiatively driven rotating convection was recently shown to obey these additional scaling predictions based on further processing of the experimental data from Ref. [30], together with a suite of Direct Numerical Simulations of rotating radiatively driven convection using the solver Coral [63].

4. Conclusion

Radiatively driven convection provides an efficient way to achieve diffusivity-free convection in the laboratory. At the theoretical level, radiatively driven convection in the horizontally infinite plane layer is well-suited for theoretical studies, from linear stability analysis to upper-bound theory. This relative simplicity also makes radiatively driven convection well-suited to include the additional physical ingredients encountered in geophysical and astrophysical contexts, such as rotation or magnetic field. As an example, the rapidly rotating radiatively driven convection experiment has led to the first experimental observation of the diffusivity-free GT regime of

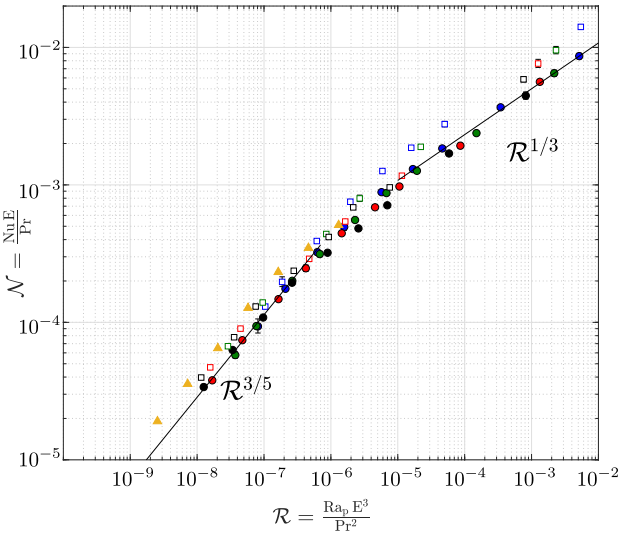

Figure 5. Diffusivity-free Nusselt number $\mathscr{N}$ as a function of the diffusivity-free flux-based Rayleigh number $\mathscr{R}$ for various fluid heights: blue, $H = 10$ cm, $Ra_P \simeq 2.5.10^{10}$; green, $H = 15$ cm, $Ra_P \simeq 1.3.10^{11}$; red, $H = 20$ cm, $Ra_P \simeq 3.5.10^{11}$; black, $H = 25$ cm, $Ra_P \simeq 9.10^{11}$. The dimensionless absorption length is $\ell/H = 0.024$ (filled circles) or $\ell/H = 0.048$ (open squares). The triangles are DNS data for $Ra_P = 10^{12}$, $Pr = 7$, and $\ell/H = 0.048$ (see Ref. [30]). In the rapidly rotating regime $\mathscr{R} \lesssim 3.10^{-7}$, the master curve agrees closely with the geostrophic turbulence scaling prediction $\mathscr{N} \sim \mathscr{R}^{3/5}$, shown as an eye guide. Experimental and numerical error bars are visible when larger than the symbol size.

rapidly rotating convection. Magnetic field could be the next ingredient to add, for instance by designing a radiatively driven liquid metal convection experiment driven by induction heating.

While we believe radiatively driven convection is interesting in itself, independently of RB convection, an intriguing question is whether the two systems can be related at the quantitative level. Can one infer the asymptotic behavior of the latter setup based on measurements performed using the former setup? Is there any link between the diffusivity-free regimes potentially arising in both systems? We are currently investigating this issue further and hope to report on it soon.

Declaration of interests

The authors do not work for, advise, own shares in, or receive funds from any organization that could benefit from this article, and have declared no affiliations other than their research organizations.

References

[1] D. J. Stevenson, "Turbulent thermal convection in the presence of rotation and a magnetic field: A heuristic theory", *Geophys. Astrophys. Fluid Dyn.* **12** (1979), no. 1, pp. 139–169.

[2] J. Marshall and F. Schott, "Open-ocean convection: Observations, theory, and models", *Rev. Geophys.* **37** (1999), no. 1, pp. 1–64.

[3] J. M. Aurnou, M. A. Calkins, J. S. Cheng, et al., "Rotating convective turbulence in Earth and planetary cores", *Phys. Earth Planet. Inter.* **246** (2015), pp. 52–71.

[4] M. F. De Jong and L. De Steur, "Strong winter cooling over the Irminger Sea in winter 2014–2015, exceptional deep convection, and the emergence of anomalously low SST", *Geophys. Res. Lett.* **43** (2016), no. 13, pp. 7106–7113.

[5] K. M. Soderlund, "Ocean dynamics of outer solar system satellites", *Geophys. Res. Lett.* **46** (2019), no. 15, pp. 8700–8710.

[6] B. W. Hindman, N. A. Featherstone and K. Julien, "Morphological Classification of the Convective Regimes in Rotating Stars", *Astrophys. J.* **898** (2020), no. 2, p. 120.

[7] S. Bire, W. Kang, A. Ramadhan, J.-M. Campin and J. Marshall, "Exploring ocean circulation on icy moons heated below", *J. Geophys. Res. Planets* **127** (2022), no. 3, article no. e2021JE007025.

[8] U. Frisch, *Turbulence: The Legacy of A.N. Kolmogorov*, Cambridge University Press, 1995.

[9] B. Castaing, G. Gunaratne, F. Heslot, et al., "Scaling of hard thermal turbulence in Rayleigh–Bénard convection", *J. Fluid Mech.* **204** (1989), pp. 1–30.

[10] S. Cioni, S. Ciliberto and J. Sommeria, "Strongly turbulent Rayleigh—Bénard convection in mercury: comparison with results at moderate Prandtl number", *J. Fluid Mech.* **335** (1997), pp. 111–140.

[11] A. Naert, T. Segawa and M. Sano, "High-Reynolds-number thermal turbulence in mercury", *Phys. Rev. E* **56** (1997), no. 2, R1302–R1305.

[12] X. Chavanne, F. Chillà, B. Chabaud, B. Castaing and B. Hébral, "Turbulent Rayleigh-–Bénard convection in gaseous and liquid He", *Phys. Fluids* **13** (2001), no. 5, article no. 1300.

[13] P.-E. Roche, F. Gauthier, R. Kaiser and J. Salort, "On the triggering of the Ultimate Regime of convection", *New J. Phys.* **12** (2010), no. 8, article no. 085014.

[14] X. He, D. Funfschilling, H. Nobach, E. Bodenschatz and G. Ahlers, "Transition to the Ultimate State of Turbulent Rayleigh–Bénard Convection", *Phys. Rev. Lett.* **108** (2012), no. 2, article no. 024502.

[15] C. R. Doering, "Absence of Evidence for the Ultimate State of Turbulent Rayleigh–Bénard Convection", *Phys. Rev. Lett.* **124** (2020), no. 22, article no. 229401.

[16] M. Gibert, H. Pabiou, F. Chillà and B. Castaing, "High-Rayleigh-Number Convection in a Vertical Channel", *Phys. Rev. Lett.* **96** (2006), no. 8, article no. 084501.

[17] M. Gibert, H. Pabiou, J.-C. Tisserand, B. Gertjerenken, B. Castaing and F. Chillà, "Heat convection in a vertical channel: Plumes versus turbulent diffusion", *Phys. Fluids* **21** (2009), no. 3, article no. 035109.

[18] J.-C. Tisserand, M. Creyssels, M. Gibert, B. Castaing and F. Chillà, "Convection in a vertical channel", *New J. Phys.* **12** (2010), no. 7, article no. 075024.

[19] M. R. Cholemari and J. H. Arakeri, "Axially homogeneous, zero mean flow buoyancy-driven turbulence in a vertical pipe", *J. Fluid Mech.* **621** (2009), pp. 69–102.

[20] S. S. Pawar and J. H. Arakeri, "Two regimes of flux scaling in axially homogeneous turbulent convection in vertical tube", *Phys. Rev. Fluids* **1** (2016), no. 4, article no. 042401.

[21] Y. Shen, P. Tong and K.-Q. Xia, "Turbulent Convection over Rough Surfaces", *Phys. Rev. Lett.* **76** (1996), no. 6, pp. 908–911.

[22] S. Ciliberto and C. Laroche, "Random Roughness of Boundary Increases the Turbulent Convection Scaling Exponent", *Phys. Rev. Lett.* **82** (1999), no. 20, pp. 3998–4001.

[23] Y.-B. Du and P. Tong, "Turbulent thermal convection in a cell with ordered rough boundaries", *J. Fluid Mech.* **407** (2000), pp. 57–84.

[24] P.-E. Roche, B. Castaing, B. Chabaud and B. Hébral, "Observation of the 1/2 power law in Rayleigh–Bénard convection", *Phys. Rev. E* **63** (2001), no. 4, article no. 045303.

[25] X.-L. Qiu, K.-Q. Xia and P. Tong, "Experimental study of velocity boundary layer near a rough conducting surface in turbulent natural convection", *J. Turbul.* **6** (2005), article no. N30.

[26] J.-C. Tisserand, M. Creyssels, Y. Gasteuil, H. Pabiou, M. Gibert, B. Castaing and F. Chillà, "Comparison between rough and smooth plates within the same Rayleigh—Bénard cell", *Phys. Fluids* **23** (2011), no. 1, article no. 015105.

[27] E. Rusaouën, O. Liot, B. Castaing, J. Salort and F. Chillà, "Thermal transfer in Rayleigh-–Bénard cell with smooth or rough boundaries", *J. Fluid Mech.* **837** (2018), pp. 443–460.

[28] S. Lepot, S. Aumaître and B. Gallet, "Radiative heating achieves the ultimate regime of thermal convection", *Proc. Natl. Acad. Sci. USA* **115** (2018), no. 36, pp. 8937–8941.

[29] V. Bouillaut, S. Lepot, S. Aumaître and B. Gallet, "Transition to the ultimate regime in a radiatively driven convection experiment", *J. Fluid Mech.* **861** (2019), article no. R5.

[30] V. Bouillaut, B. Miquel, K. Julien, S. Aumaître and B. Gallet, "Experimental observation of the geostrophic turbulence regime of rapidly rotating convection", *Proc. Natl. Acad. Sci. USA* **118** (2021), no. 44, article no. e2105015118.

[31] E. A. Spiegel and G. Veronis, "On the Boussinesq approximation for a compressible fluid", *Astrophys. J.* **131** (1960), pp. 442–447.

[32] L. N. Howard, "Heat transport by turbulent convection", *J. Fluid Mech.* **17** (1963), no. 3, pp. 405–432.

[33] E. A. Spiegel, "A Generalization of the Mixing-Length Theory of Turbulent Convection.", *Astrophys. J.* **138** (1963), pp. 216–225.

[34] E. A. Spiegel, "Convection in Stars I. Basic Boussinesq Convection", *Annu. Rev. Astron. Astrophys.* **9** (1971), no. 1, pp. 323–352.
[35] R. H. Kraichnan, "Turbulent Thermal Convection at Arbitrary Prandtl Number", *Phys. Fluids* **5** (1962), no. 11, pp. 1374–1389.
[36] Y.-C. Xie and K.-Q. Xia, "Turbulent thermal convection over rough plates with varying roughness geometries", *J. Fluid Mech.* **825** (2017), pp. 573–599.
[37] X. Zhu, R. J. A. M. Stevens, R. Verzicco and D. Lohse, "Roughness-facilitated local 1/2 scaling does not imply the onset of the ultimate regime of thermal convection", *Phys. Rev. Lett.* **119** (2017), no. 15, article no. 154501.
[38] S. Toppaladoddi, A. J. Wells, C. R. Doering and J. S. Wettlaufer, "Thermal convection over fractal surfaces", *J. Fluid Mech.* **907** (2021), article no. A12.
[39] B. Miquel, "Coral: a parallel spectral solver for fluid dynamics and partial differential equations", *J. Open Source Softw.* **6** (2021), no. 65, article no. 2978.
[40] S. Kazemi, R. Ostilla-Mónico and D. Goluskin, "Transition between boundary-limited scaling and mixing-length scaling of turbulent transport in internally heated convection", *Phys. Rev. Lett.* **129** (2022), no. 2, article no. 024501.
[41] B. Miquel, V. Bouillaut, S. Aumaître and B. Gallet, "On the role of the Prandtl number in convection driven by heat sources and sinks", *J. Fluid Mech.* **900** (2020), article no. R1.
[42] W. V. R. Malkus, "The heat transport and spectrum of thermal turbulence", *Proc. R. Soc. Lond., Ser. A* **225** (1954), no. 1161, pp. 196–212.
[43] C. R. Doering and P. Constantin, "Variational bounds on energy dissipation in incompressible flows. III. Convection", *Phys. Rev. E* **53** (1996), no. 6, pp. 5957–5981.
[44] F. H. Busse, "On Howard's upper bound for heat transport by turbulent convection", *J. Fluid Mech.* **37** (1969), pp. 457–477.
[45] B. Miquel, S. Lepot, V. Bouillaut and B. Gallet, "Convection driven by internal heat sources and sinks: Heat transport beyond the mixing-length or 'ultimate' scaling regime", *Phys. Rev. Fluids* **4** (2019), no. 12, article no. 121501.
[46] V. Bouillaut, B. Flesselles, B. Miquel, S. Aumaître and B. Gallet, "Velocity-informed upper bounds on the convective heat transport induced by internal heat sources and sinks", *Philos. Trans. R. Soc. Lond., Ser. A* **380** (2022), no. 2225, article no. 20210034.
[47] B. Song, G. Fantuzzi and I. Tobasco, "Bounds on heat transfer by incompressible flows between balanced sources and sinks", *Phys. D: Nonlinear Phenom.* **444** (2023), article no. 133591.
[48] E. M. King, S. Stellmach, J. Noir, U. Hansen and J. M. Aurnou, "Boundary layer control of rotating convection systems", *Nature* **457** (2009), no. 7227, pp. 301–304.
[49] R. P. J. Kunnen, "The geostrophic regime of rapidly rotating turbulent convection", *J. Turbul.* **22** (2021), no. 4-5, pp. 267–296.
[50] L. Terrien, B. Favier and E. Knobloch, "Suppression of wall modes in rapidly rotating Rayleigh–Bénard convection by narrow horizontal fins", *Phys. Rev. Lett.* **130** (2023), no. 17, article no. 174002.
[51] E. M. King, S. Stellmach and J. M. Aurnou, "Heat transfer by rapidly rotating Rayleigh—Bénard convection", *J. Fluid Mech.* **691** (2012), pp. 568–582.
[52] P. Joshi, H. Rajaei, R. P. J. Kunnen and H. J. H. Clercx, "Heat transfer in rotating Rayleigh–Bénard convection with rough plates", *J. Fluid Mech.* **830** (2017), R3.
[53] V. K. Tripathi and P. Joshi, "Regimes in rotating Rayleigh– Bénard convection over rough boundaries", *J. Fluid Mech.* **982** (2024), article no. A15.
[54] F. Toselli, S. Musacchio and G. Boffetta, "Effects of rotation on the bulk turbulent convection", *J. Fluid Mech.* **881** (2019), pp. 648–659.
[55] C. Liu, M. Sharma, K. Julien and E. Knobloch, "Fixed-flux Rayleigh—Bénard convection in doubly periodic domains: generation of large-scale shear", *J. Fluid Mech.* **979** (2024), article no. A19.
[56] K. Julien, E. Knobloch and J. Werne, "A New Class of Equations for Rotationally Constrained Flows", *Theor. Comput. Fluid Dyn.* **11** (1998), no. 3-4, pp. 251–261.
[57] K. Julien, E. Knobloch, R. Milliff and J. Werne, "Generalized quasi-geostrophy for spatially anisotropic rotationally constrained flows", *J. Fluid Mech.* **555** (2006), pp. 233–274.
[58] K. Julien, E. Knobloch, A. M. Rubio and G. M. Vasil, "Heat Transport in Low-Rossby-Number Rayleigh–Bénard Convection", *Phys. Rev. Lett.* **109** (2012), no. 25, article no. 254503.
[59] K. Julien, A. M. Rubio, I. Grooms and E. Knobloch, "Statistical and physical balances in low Rossby number Rayleigh-–Bénard convection", *Geophys. Astrophys. Fluid Dyn.* **106** (2012), no. 4-5, pp. 392–428.
[60] A. J. Barker, A. M. Dempsey and Y. Lithwick, "Theory and simulations of rotating convection", *Astrophys. J.* **791** (2014), no. 1, article no. 13.
[61] S. Stellmach, M. Lischper, K. Julien, et al., "Approaching the asymptotic regime of rapidly rotating convection: boundary layers versus interior dynamics", *Phys. Rev. Lett.* **113** (2014), no. 25, article no. 254501.

[62] J. Song, O. Shishkina and X. Zhu, "Scaling regimes in rapidly rotating thermal convection at extreme Rayleigh numbers", *J. Fluid Mech.* **984** (2024), article no. A45.

[63] G. Hadjerci, V. Bouillaut, B. Miquel and B. Gallet, "Rapidly rotating radiatively driven convection: experimental and numerical validation of the 'geostrophic turbulence' scaling predictions", *J. Fluid Mech.* **998** (2024), article no. A9.

[64] J. M. Aurnou, S. Horn and K. Julien, "Connections between nonrotating, slowly rotating, and rapidly rotating turbulent convection transport scalings", *Phys. Rev. Res.* **2** (2020), no. 4, article no. 043115.